to the metastatic potential of its individual cells. This high degree of heterogeneity is probably attributable to the fact that the B16 melanoma has existed as a transplanted tumor for more than 20 years. It is quite likely that many variants would arise during this period by the process of mutation and selection and by epigenetic mechanisms (*4*). In addition, the process of metastasis is a complex one with many sequential steps. It begins with the invasion of tissues and vessels by cells originating in the primary cancer. After their entry into the circulation, most cells are arrested in the first capillary bed encountered, but some continue and are trapped in other organs. After this arrest, the tumor cells must invade the parenchyma, proliferate, establish a vascular supply, and escape host defense mechanisms in order to develop into secondary foci. A cell that acquires an increased ability to survive any one of these steps would be viewed as having an increased metastatic potential. Thus, there are probably many different pathways by which a cell could acquire an increased or decreased capacity to form a new colony at a distant site.

The possible existence of highly metastatic variant cells within a primary tumor may have important consequences for cancer therapy. Efforts to design effective therapeutic agents and procedures should be directed toward the few, albeit fatal, metastatic subpopulations. Continuing efforts to eradicate the bulk of neoplastic cells, without regard to their biological behavior, are likely to be unproductive. Perhaps the highly metastatic clones described in our study would be useful tools for testing new therapeutic approaches to cancer.

ISAIAH J. FIDLER
MARGARET L. KRIPKE
*Basic Research Program, National Cancer Institute Frederick Cancer Research Center, Frederick, Maryland 21701*

### References and Notes

1. I. Zeidman, *Cancer Res.* **17**, 157 (1957); E. R. Fisher and B. Fisher, *Arch. Pathol.* **83**, 321 (1967); I. J. Fidler, in *Cancer*, F. F. Becker, Ed. (Plenum, New York, 1976), vol. 4, pp. 101–131.
2. I. J. Fidler, *J. Natl. Cancer Inst.* **45**, 775 (1970).
3. ———, *Nature (London) New Biol.* **242**, 148 (1973); *Cancer Res.* **35**, 218 (1975).
4. P. C. Nowell, *Science* **194**, 23 (1976).
5. S. E. Luria and M. Delbrück, *Genetics* **28**, 491 (1943).
6. Cells were grown on plastic in Eagle's minimum essential medium supplemented with 10 percent fetal calf serum, vitamin solution, sodium pyruvate, nonessential amino acids, penicillin-streptomycin, and L-glutamine, designated complete minimum essential medium (CMEM) (Flow Laboratories, Rockville, Md.).
7. A 1 percent mixture of agarose was prepared in distilled, deionized sterile $H_2O$. The mixture was boiled and agitated, then cooled to 37°C and mixed with equal volume of double strength CMEM. A layer of CMEM and agarose was placed in a petri dish (120 by 20 mm) and the remaining mixture was kept warm at 37°C. A single cell suspension of the B16 melanoma in CMEM was adjusted to contain 2000 viable cells per milliliter. The cell suspension was diluted with an equal amount of the agarose and CMEM mixture. One milliliter of the final suspension (1000 cell/ml) was added to each petri dish, and the mixture was allowed to harden. The dishes were incubated at 37°C (5 percent $CO_2$) overnight. After that time, the dishes were examined under an inverted microscope and the positions of *isolated single* cells were noted and marked. Single cells were removed with a Pasteur pipette and placed in a Microtest II well (Falcon Plastics). Twelve hours later the wells were examined, and those with an attached single cell were identified. Tumor colonies resulting from these single cells were propagated and serially transferred to vessels of increasing size.
8. S. Siegel, *Nonparametric Statistics for the Behavioral Sciences* (McGraw-Hill, New York, 1956), pp. 116–126.
9. We thank Z. Barnes and J. Connor for technical assistance. Supported by National Cancer Institute contract N01-C0-25423 with Litton Bionetics, Inc.

16 May 1977

## Phi Bodies: Peroxidatic Particles that Produce Crystalloidal Cellular Inclusions

Abstract. *Unique, spindle-shaped particles ($\phi$ bodies) and rods with peroxidatic activity are found in certain epithelial cells of normal mice, clofibrate-fed rats, and in leukemic leukocytes. The ellipsoidal shape of $\phi$ bodies apparently results from the deformation of spherical granules by extrusion of axial crystalloid that subsequently fragments into rods.*

While studying the abundant peroxisomes in mouse salivary gland distal duct luminal epithelial cells with light microscopic histocytochemical methods for the direct demonstration of their isocitrate dehydrogenase (*1*) and catalase, we observed (*2*) enzyme-reactive rods as well as filaments of different dimensions (Fig. 1). Study of the size and distribution of these rods and filaments suggested that they could not be microorganisms (*3*). This was confirmed by correlative studies with the electron microscope, which also demonstrated that these structures were crystalloid rather than crystalline.

In our earliest studies of these rods we observed spindle-shaped particles (Figs. 1 to 3) which, at first, were thought to consist of microbodies superimposed on rods. At this time, neither the change in conformation of the peroxisome from spheroidal to ellipsoidal nor the increase in size that accompanies its transformation to the $\phi$ body had been recognized. Indeed, the elucidation of the $\phi$ body as a unique and distinct cellular particle visible with the light microscope in histocytochemical enzyme preparations was delayed by our ability to resolve several of these putative spindle-shaped particles into rods superimposed on peroxisomes with the light microscope.

Study of the specimen shown in Fig. 1, however, suggested that a considerably higher incidence of these particles than might be expected from the fortuity of superimposition could be found in certain areas of the ductal epithelium. Further study of this specimen revealed that the centers of almost all of these unique spindle-shaped particles, which could not be resolved with the light microscope as being due to overlapping peroxisomes and rods, were ellipsoidal rather than spherical. It was also noted at this time that the rods or filaments which extruded from the poles of the $\phi$ body invariably appeared to coincide with the major axis of its ellipsoidal center. The $\phi$ body centers were also generally larger than nearby spheroidal microbodies.

These observations led to the hypothesis that the deformation of the spherical microbody to an ellipsoidal shape and its increase in size could result from internal pressure exerted by crystalloid growing in the centers of the relatively small numbers of transforming microbodies prior to and during the extrusion of the same material from their poles. This proposed mechanism is similar to the "tent-pole" effect proposed for the protein crystalloid of immature eosinophil granules by which their spherical contours become angulated (*4*). A similar effect appears to account for the population of ellipsoidal azurophilic granules of normal neutrophilic promyelocytes which have an axial band of crystalloid (*5*).

Several other considerations also tended to relate $\phi$ bodies to free rods observed in the luminal epithelial cells of the distal ducts of mouse salivary glands. Light microscopic study of the submandibular glands of many strains of mice and several strains of rats revealed that, although nonparticulate catalase and peroxisomes were prominent in the distal salivary gland duct cells of all strains, $\phi$ bodies were observed only in the tissues of the rodent strains that contained catalase-positive rods or filaments and vice versa (*3*). This similarity in distribution, although a very important consideration, was perhaps not as significant as the frequent observation with the light

microscope (Figs. 3 and 4) of segmentation of the axial processes of the $\phi$ bodies. This was confirmed by occasional electron microscopic observations (Fig. 5B). Although detachment was usually observed at the proximal end (Fig. 5B) where the rods extruded from the center, it was occasionally observed more distally (Fig. 3). The register of the detached or extruded segments in linear array was also observed in several cases (Fig. 4). When the parent $\phi$ body could be located, it was observed that the detached segments were almost invariably aligned along the major axis of the elliptical $\phi$ body center, suggesting that the extrusion of segments could occur with some rapidity.

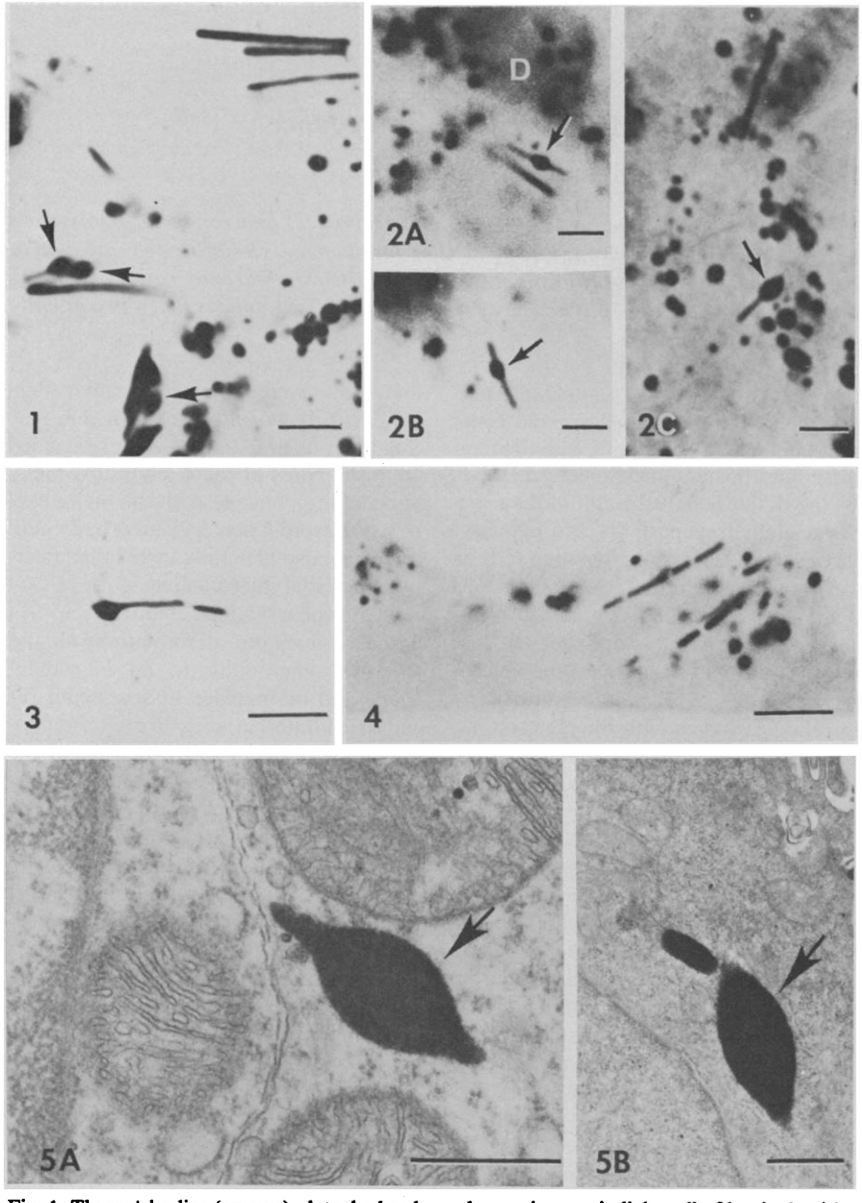


Fig. 1. Three $\phi$ bodies (arrows), detached rods, and peroxisomes in light cell of luminal epithelium of Wharton's duct. Cryostat section. Light micrograph of glutaraldehyde-fixed salivary gland tissue, incubated for catalase demonstration (*1*), then osmicated. The marker represents 5 $\mu$m. Fig. 2. Phi bodies (arrows) of various conformations in ductal epithelial cells. Cryostat sections. Light micrographs of glutaraldehyde-fixed salivary gland tissue, incubated for catalase demonstration (*1*), then osmicated. The marker represents 5 $\mu$m. (A) A $\phi$ body and adjacent rod in light cell. Note cytoplasmic activity in dark cell (D) and numerous peroxisomes. (B) A $\phi$ body with processes of unequal lengths. (C) A $\phi$ body with thin, lightly stained process. Fig. 3. A $\phi$ body with single, thick axial process showing distal break. Cryostat section. Light micrograph of glutaraldehyde-fixed salivary gland tissue, incubated for catalase demonstration (*1*), then osmicated. The marker represents 5 $\mu$m. Fig. 4. Rod segments in register, suggesting rapidity of sequential extrusion. In this section (2 $\mu$m) the tissue was embedded in plastic. Light micrograph of glutaraldehyde-fixed salivary gland tissue, incubated for catalase demonstration (*1*), then osmicated. The marker represents 5 $\mu$m. Fig. 5. Phi bodies (arrows) in salivary ductal epithelial cells. The reaction product obscures the equatorial crystalloid. Fixed and incubated with DAB medium; counterstained with uranyl acetate and lead citrate. The marker represents 0.5 $\mu$m. (A) This holotypic $\phi$ body has an axial process protruding from each end. (B) A $\phi$ body with detached axial process.

All of the evidence cited above to link the $\phi$ body to the filaments or rods is merely circumstantial. The proof that the $\phi$ body gives birth to the detached or segmented rods was obtained from electron microscopic studies of osmium-fixed preparations of excised Wharton's duct of mouse submandibular gland. Here the substructure was not obscured by the enzyme histochemical reaction product, and a band of equatorial crystalloid was revealed in those ellipsoidal microbodies that were transforming into $\phi$ bodies (Fig. 6). In $\phi$ bodies, where the equatorial crystalloid was already protruding through the pole of ellipsoidal central portion (Figs. 5 and 6, B to E), it always coincided with the principal axis of the ellipsoidal $\phi$ body center. Although observation of the true length of the extruding crystalloid processes from the center of the $\phi$ body was limited by the narrow plane of sectioning for electron microscopy, extrusion as the mechanism for the formation of the detached rods is confirmed by comparison (*6*) of the crystalloid of the $\phi$ body with that of the free rods (Fig. 7). This revealed that the periodic substructure of the crystalloid of the $\phi$ bodies and the detached rods is identical, and that it consists of parallel tubules approximately 130 Å in diameter connected by dense, lateral cross-links approximately 160 Å apart. The long axis of the tubule is invariably coincident with the long axis of the $\phi$ body crystalloid or of the detached rod. In cross section (Fig. 6G), the tubules appeared to form a random array with no apparent secondary order. The cross-linking of the parallel tubules accounts for the woven or herringbone pattern observed in electron micrographs of longitudinal sections of the crystalloid in both the detached rods and $\phi$ bodies.

The catalase-positive rods and $\phi$ bodies, like microbodies in salivary gland distal duct luminal epithelial cells of mice, vary in size. The ellipsoidal centers of $\phi$ bodies vary from approximately 0.5 to 1.5 $\mu$m along their major axes. The processes or detached rods and filaments may be much larger and occasionally extend across an entire cell (*2, 3*). Although the processes of a $\phi$ body are frequently of approximately the same length, $\phi$ bodies having only one process or processes of quite unequal lengths are also commonly observed (Fig. 2). The axial processes (like the detached rods) vary from

very fine filaments to rather robust rods, and there is no apparent relation between the size of the process and that of the $\phi$ body center. Yet there appeared, by light microscopy, to be a relation of the length of the process to its robustness, the longer processes being more robust. The frequent appearance of short unilateral, very fine filamentous processes on large $\phi$ body centers also suggests that a $\phi$ body may produce successive generations of rods.

The intensity of catalase staining of the processes and of the detached rods appears to be related to their size, but this is not always the case. Even the finest filaments and processes have sufficient catalase activity to enable their facile detection with the light microscope; they do not have nearly as much isocitrate dehydrogenase activity, however. This could mean that catalase is one of the first paracrystalline proteins to appear in the core of the mouse salivary gland duct luminal epithelial cell microbodies transforming into $\phi$ bodies. Support for this is received from several light microscopic observations of greater catalase activity in the equatorial band of crystalloid and in the processes than in the matrix of the $\phi$ body center. Although this band could be an artifact due to refraction, our observations suggest that the crystalloid core of the transforming microbodies differs from other animal microbodies having polytubular crystalloid cores. The latter are believed to be composed of uricase (*7*) and other proteins, whereas the crystalloid core of plant microbodies is believed to consist of catalase (*8*). The catalase in the core of plant leaf peroxisomes may represent the progressive coacervation or crystallization of catalase from the microbody matrix (*9*). Such an accretion of catalase from the matrix of the $\phi$ body center could account for the greater catalase activity observed in its equatorial band. Similarly, there could be a progressive coacervation of catalase from the cytoplasmic pool in the mouse distal duct luminal epithelial cells to the new processes of the $\phi$ body and the smaller detached rods, which could account for their growth and the greater enzyme activity of the larger processes and rods. There are two populations of cells with respect to cytoplasmic catalase activity observed in this luminal epithelium, light and dark cells, and the detached $\phi$ bodies and rods are usually seen in the former (*2*).

The only other enzyme studied in the rods and $\phi$ bodies is isocitrate dehydrogenase, which is observed in a much more limited population of these as well as in fewer of the neighboring peroxisomes. The crystalloid cores of the transforming peroxisomes and of the $\phi$ bodies may contain small amounts of a number of coacervated paracrystalline proteins in addition to catalase and isocitrate dehydrogenase. The fact that only one polytubular substructure is observed in the electron microscopic studies of the crystalloid cores suggests, however, that catalase is the principal structural protein while the quantities of other proteins are relatively small. In studies on the crystallization of purified catalase, it was shown that, although catalase usually forms crystals, the presence of certain substances may induce the formation of paracrystalline tubules (*10*).

The transformation of microbodies into tubular structures resembling $\phi$ bodies has been observed in many, almost exclusively, ultrastructural studies (*11*). These transformations, occasionally accompanied by microbody proliferation and increased catalase synthesis, are more usually observed in tissues of rodents bearing tumors or treated with certain drugs. In some cases, their relationship to catalase-positive rods in the cytoplasm has even been noted. The emphasis in these studies, however, was on the transformation of the microbody matrix into tubular structures rather than on the transformation of the peroxisome itself into a specialized form which has a function in producing detached paracrystalline cellular inclusions. The tubules of these transformed peroxisomes were generally of greater diameter than those seen in our studies. Although $\phi$ bodies can be seen in their light micrographs, the characteristic light microscopic profile of the $\phi$ body was not described in these studies. In at least one case, however, the ultrastructural features of a similar transformed microbody were rather accurately described (*12*). Similar light and electron microscopic studies of tissues from male hypophysectomized rats fed high doses of clofibrate have revealed the induction of rods and $\phi$ bodies in proximal convoluted tubular epithelial cells of kidney. The unit tubules of the crystalloid core are 1200 Å in diameter in both the $\phi$ bodies and detached rods.

Microbodies were previously observed in salivary gland cells (*13*), but transforming forms have been infrequently reported. In cat submandibular ductal cells, deformed, crystalloid-containing microbodies, analogous to $\phi$ bod-

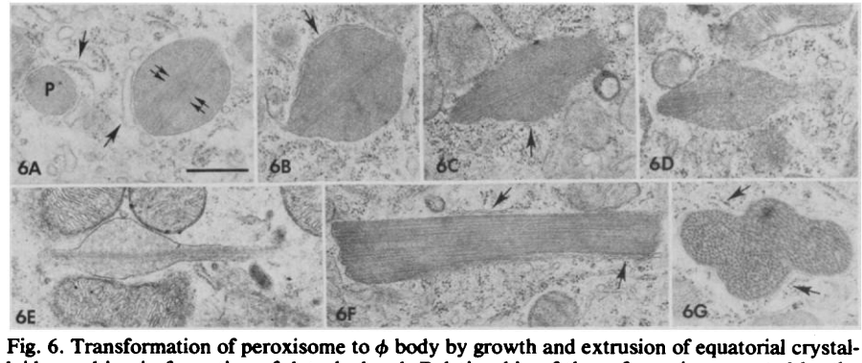


Fig. 6. Transformation of peroxisome to $\phi$ body by growth and extrusion of equatorial crystalloid, resulting in formation of detached rod. Relationship of these forms is supported by the presence of a limiting membrane and association with endoplasmic reticulum (arrows). Fixed solely by immersion in 1 percent $OsO_4$, except (E) which was fixed with glutaraldehyde, osmicated, then amplified by bridging with thiocarbohydrazide and $OsO_4$ (*22*) prior to embedment. Counterstained with uranyl acetate and lead citrate. Marker, 0.5 $\mu$m. (A) Note smaller spherical peroxisome (*P*) adjacent to transforming peroxisome with axial crystalloid (double arrows). (B to E) Stages in extrusion of axial crystalloid from both ends of the $\phi$ body center. (F and G) Detached rods in longitudinal (F) and cross section (G).

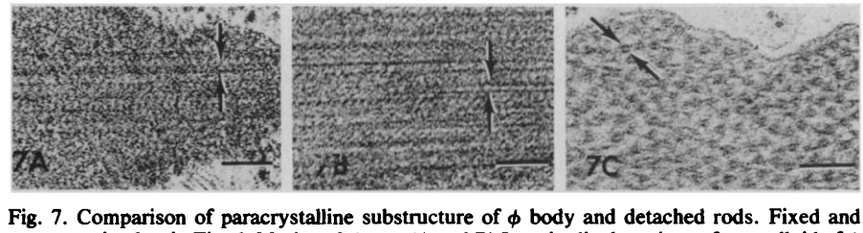


Fig. 7. Comparison of paracrystalline substructure of $\phi$ body and detached rods. Fixed and counterstained as in Fig. 6. Marker, 0.1 $\mu$m. (A and B) Longitudinal sections of crystalloid of $\phi$ body and rod, enlarged from Fig. 6, C and F, respectively. Tubule diameter of 130 Å is evident (arrows). Cross-links result in herringbone appearance. (C) Rod in cross section, enlarged from Fig. 6G. Diameter of tubule, 130 Å (arrows).

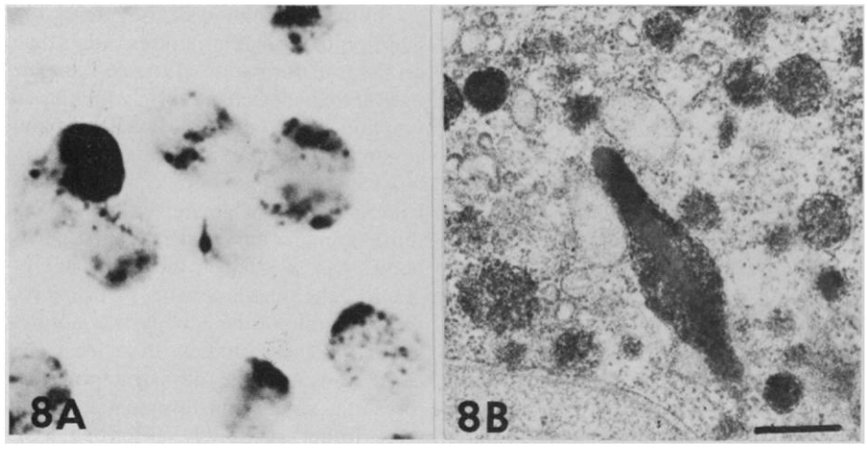


Fig. 8. Micrographs of $\phi$ bodies in peripheral leukocytes of patient E.S., a 43-year-old male, with acute myelogenous leukemia (*19*). The leukocyte preparation was treated for catalase demonstration as described above. (A) Light micrograph, × 1200. (B) Electron micrograph. Marker, 0.5 $\mu$m.

ies, have been observed (*14*). Moreover, $\phi$ bodies are present in human labial salivary gland acinar cells, although their relation to microbodies was not observed (*15*). In rabbit kidney proximal convoluted tubular epithelial cells, $\phi$ bodies have been observed (*16*) that are identical to those we report, even with respect to the periodicity of the finely tubular substructure. These observations suggest that $\phi$ bodies—although less frequently observed than catalase-positive rods, which in turn are not nearly as prevalent as microbodies—may be present in many types of animal cells containing microbodies.

Various crystalloid cellular inclusions apparently can be derived from the rough endoplasmic reticulum, mitochondria, and lysosomes as well (*17*). The Auer rods of leukemic leukocytes, which have peroxidatic activity, are generally thought to arise by the fusion of the leukocytic azurophilic granules. However, structures resembling $\phi$ bodies, which have an axial crystalloid composed of similar tubules (*18*), have been reported in leukocytes of a number of leukemic patients. With the light microscope, numerous $\phi$ bodies were readily observed by virtue of their peroxidatic activity (Fig. 8) in the leukocytes of a patient with acute myelogenous leukemia (*19*). They could be responsible for the formation of Auer rods by a mechanism similar to that observed for the catalase-positive rods in the epithelial cells.

Support for this hypothesis may follow from the observations (*20*) that catalase is present in increased amounts in azurophilic or primary granules of leukocytes in myelocytic or myelogenous leukemias (rods present) while in acute lymphocytic leukemia (rods absent) it is very low. This would mean that the $\phi$ body is involved in packaging or sequestering excess enzyme for a specific purpose, such as storage or elimination.

This new cellular particle was discovered by light microscopic study of specimens treated for the direct demonstration of enzymes by histocytochemical methods (*1*). It was then characterized by correlative studies with the light and electron microscopes. The less desirable disruptive biochemical fractionation techniques, which assumed a dominant role in the elucidation of the lysosome and the peroxisome (*21*), were not applicable because of the general paucity of this particle and its relative prevalence in cells or epithelia which lend themselves to direct microscopic exploration.

The transformation of the peroxisome and the azurophilic granule (generally considered to be a lysosome) into $\phi$ bodies establishes the uniqueness of this new cell particle. It also suggests that there may be a closer relation between these progenitor particles than commonly believed.

JACOB S. HANKER
DWIGHT K. ROMANOVICZ
*Dental Research Center, School of Dentistry, University of North Carolina, Chapel Hill 27514*

### References and Notes

1. In the light microscopic histocytochemical methods for isocitrate dehydrogenase and catalase we used osmiophilic reagents [J. S. Hanker, A. R. Seaman, L. P. Weiss, H. Ueno, R. A. Bergman, A. M. Seligman, *Science* **146**, 1039 (1964)]. Since the osmium black end products are electron-opaque as well as visible, these methods may also be adapted for electron microscopy. The isocitrate dehydrogenase procedure was developed by us (J. S. Hanker, P. E. Yates, D. K. Romanovicz, in preparation). The method for demonstrating catalase is based on its ability to catalyze the peroxidation of the osmiophilic reagent 3,3'-diaminobenzidine (DAB), which was introduced into histocytochemistry for peroxidase demonstration [R. C. Graham, Jr., and M. J. Karnovsky, *J. Histochem. Cytochem.* **14**, 291 (1966)]. The incubation media for the demonstration of catalase contained DAB [A. B. Novikoff and S. Goldfischer, *ibid.* **17**, 675 (1969); M. A. Venkatachalam, M. H. Soltani, H. D. Fahimi, *J. Cell Biol.* **46**, 168 (1970)]. All of the above procedures could be modified after incubation for light microscopy by replacing postosmication by briefly rinsing the preparation in tris buffer and treating with 0.5 percent $Cu(NO_3)_2$ in 0.5*M* tris-HCl buffer (*p*H 7.6). This treatment intensifies and darkens the sites of catalase staining with DAB. In contrast, lipid constituents and membranes ordinarily stained by osmication and structures rich in nucleic acids or sulfated mucopolysaccharides, such as mast cell granules which have a great affinity for DAB monomer, are not stained as with postosmication. Since the chelated DAB reaction products may have some solubility in organic solvents, this procedure is modified for electron microscopy [D. K. Romanovicz and J. S. Hanker, *Histochem. J.* **9**, 317 (1977)]. The osmication is omitted and chelation is effected with uranyl acetate and lead citrate on the ultrathin section containing the polymerized DAB.
2. J. S. Hanker, J. W. Preece, E. J. Burkes, Jr., D. K. Romanovicz, *Histochem. J.*, in press.
3. J. S. Hanker, M. S. Silverman, D. K. Romanovicz, *ibid.*, in press.
4. B. D. Wetzell, R. G. Horn, S. S. Spicer, *Lab Invest.* **16**, 349 (1967).
5. D. F. Bainton, J. L. Ullyot, M. G. Farquhar, *J. Exp. Med.* **134**, 907 (1971); D. F. Bainton, L. M. Friedlander, S. B. Shohet, *Blood* **49**, 693 (1977).
6. Measurements of the crystalloid periodicities were made from enlarged electron micrographs, calibrated with a carbon grating replica (Polysciences, Inc., Warrington, Pa.) used as an external standard [R. A. Haschemeyer and R. J. Meyers, in *Principles and Techniques of Electron Microscopy*, M. A. Hayat, Ed. (Van Nostrand Reinhold, New York, 1972), vol. 2].
7. T. K. Shnitka, *J. Ultrastruct. Res.* **16**, 598 (1966).
8. E. L. Vigil, *J. Histochem. Cytochem.* **17**, 425 (1969); *Sub-Cell. Biochem.* **2**, 237 (1973).
9. S. E. Frederick and E. H. Newcomb, *J. Cell Biol.* **43**, 343 (1969).
10. N. A. Kiselev, C. L. Shpitzberg, B. K. Vainshtein, *J. Mol. Biol.* **25**, 433 (1967).
11. Z. Hruban, H. Swift, A. Slesers, *Lab. Invest.* **15**, 1884 (1966); J. Reddy and D. Svoboda, *J. Histochem. Cytochem.* **20**, 793 (1972); J. K. Reddy, *ibid.* **21**, 967 (1973); J. Reddy and D. Svoboda, *Virchows Arch. B* **14**, 83 (1973).
12. K. H. Langer, *Z. Zellforsch.* **90**, 432 (1968).
13. A. R. Hand, *J. Histochem. Cytochem.* **21**, 131 (1973).
14. A. Kidd and J. R. Garrett, personal communication.
15. B. Tandler, C. R. Denning, I. D. Mandel, A. H. Kutscher, *J. Morphol.* **127**, 383 (1969).
16. B. Kaissling, personal communication.
17. F. N. Ghadially, *Ultrastructural Pathology of the Cell* (Butterworth, London, 1975).
18. The similarities of the substructures of peroxidase-positive Auer rods of leukemic leukocytes to the catalase-positive rods observed in our study were pointed out by Dr. Aldo F. Cecio, Department of Topographic Anatomy of the University of Naples, and by several scientists of the Cancer Research Center, Academy of Medical Sciences of the U.S.S.R., and of the Institute of Oncology Problems, Ukrainian S.S.R. Academy of Sciences.
19. We thank Dr. John Laszlo of the Duke Medical Center and Dr. Joseph Moore of the Veterans Administration Hospital, Durham, N.C., for the supply and classification of the blood specimens.
20. M. Ichimaru, *J. Kyushu Hematol. Soc.* **9**, 722 (1959); E. T. Nishimura and C. Cooper, *Cancer Res.* **24**, 2386 (1974); E. T. Nishimura, G. M. Whest, H.-Y. Yang, *Lab. Invest.* **34**, 60 (1976).
21. C. de Duve, *Science* **189**, 186 (1975).
22. J. S. Hanker, C. Deb, H. L. Wasserkrug, A. M. Seligman, *ibid.* **152**, 1631 (1966).
23. Supported by PHS research grants DE 02668, DE 05087, and RR 05333. This work was presented, in part, at the plenary sessions of the Fifth International Congress of Histochemistry and Cytochemistry in Bucharest, August 1976, supported by NSF international travel grant PCM76-22977, and at the Fifth International School of Electron Microscopy, Erice, Sicily, April 1977. We thank Dr. Ronald V. Chandross for suggesting the name $\phi$ body, W. W. Ambrose and P. E. Yates for technical assistance, W. Patterson and Foister's for assistance in photography, and J. P. Goulson and C. L. James for reviewing the manuscript.

22 December 1976; revised 1 June 1977